Available online at www.sciencedirect.com
ScienceDirect
Catalysis Today 118 (2006) 416–424
CATALYSIS TODAY
www.elsevier.com/locate/cattod

# New Nb-containing SBA-3 mesoporous materials—Synthesis, characteristics, and catalytic activity in gas and liquid phase oxidation

Beata Kilos [a], Alain Tuel [b,*], Maria Ziolek [a,**], Jean-Claude Volta [b]

[a] *Adam Mickiewicz University, Faculty of Chemistry, Grunwaldzka 6, 60-780 Poznan, Poland*
[b] *Institut de Recherches sur la Catalyse, CNRS, 2 Av. Albert Einstein, 69626 Villeurbanne Cédex, France*

Available online 28 August 2006

**Abstract**

The synthesis and characterization of NbSBA-3 mesostructured materials – the first hexagonally ordered mesoporous molecular sieves without extra framework Nb-oxide phase – are described in this paper. The effect of the synthesis medium (basic or acidic) and Nb source in the efficiency of niobium incorporation is discussed. A higher Nb content in the final material is reached when Nb(V) chloride is used instead of Nb(V) ammonium trisoxalate complex in the synthesis. All NbSBA-3 materials prepared in this work are very attractive catalysts in ODH of propane and epoxidation of cyclohexene and more effective than the corresponding NbMCM-41 and NbSBA-15 catalysts.


*Keywords:* NbSBA-3; XRD; $N_2$ adsorption/desorption; UV–vis; FTIR + pyridine; ODH of propane; Epoxidation of cyclohexene

## 1. Introduction

Since the discovery of M41S mesoporous molecular sieves [1], with MCM-41 as the main representative of this family, various modifications in the synthesis of mesostructured materials have been performed. Among others, Stucky et al. [2] obtained materials denoted as SBA-3 by changing a basic synthesis medium for an acidic one. From the catalytic point of view the mesoporous solids are attractive if they are modified with desired metal species. Such a modification can be carried out in two ways, via an introduction of metal during the synthesis or via a post-synthesis treatment. Following the first route, up to now niobium has been incorporated into MCM-41 and SBA-15 structures [3–9]. However, for Si/Nb ratio 32 or 64, in most cases Nb was located not only in the walls of mesoporous channels, but also in the extra framework sites, as Nb-oxides phases. Moreover, the efficiency of niobium incorporation during the synthesis strongly depends on the structure of the final material and it is much higher for MCM-41 [3] than for the SBA-15 [5]. The main differences in the preparation of both mesoporous molecular sieves are the type of template used (ionic surfactant for MCM-41 and triblock copolymer in case of SBA-15) and the synthesis medium (basic, MCM-41 and acidic, SBA-15). Another parameter, which has to be considered, is the niobium source, which also influences the amount of metal included into the mesoporous material [10]. The question arises if the preparation of hexagonally ordered mesostructured solids with using of ionic surfactant as a template but acidic medium instead of basic one can lead to the high efficiency of Nb inclusion into the skeletal positions. Looking for the mesostructured materials free from Nb extra framework species we have followed Stucky's preparation of SBA-3 [2], introducing various Nb salts during the synthesis in acidic media.

The aim of this study was to prepare NbSBA-3 solids containing Si/Nb ratios between 32 and 128 (in the gel), to characterize their textural/structural and surface properties, and to test their activity in the gas and liquid phase oxidation of propane (ODH process) and cyclohexene, respectively.

## 2. Experimental methods

### 2.1. Synthesis of the catalysts

All SBA-3 materials were synthesised following the procedure reported originally by Stucky et al. [2]. Cetyltrimethylammonium bromide (CTAB, Aldrich) and tetraethyl

* Corresponding author.
** Corresponding author. Tel.: +48 61 829 1243; fax: +48 61 865 8008.
*E-mail addresses:* tuel@catalyse.cnrs.fr (A. Tuel), ziolek@amu.edu.pl (M. Ziolek).

0920-5861/$ – see front matter © 2006 Elsevier B.V. All rights reserved.
doi:10.1016/j.cattod.2006.07.029

orthosilicate (TEOS, Aldrich, 98%) were used as a surfactant and silica source, respectively. The surfactant was mixed with water and hydrochloric acid (37%, Prolabo). TEOS was added dropwise to the acidic CTAB solution with stirring to form a mixture with a molar ratio of: 1 $SiO_2$:0.12 CTAB:9.2 HCl:130 $H_2O$. The mixture was stirred at room temperature (24 h) to gain homogeneous solution. The samples were recovered by filtration, washed with a copious amount of water and dried at 473 K for 3 h. After calcination at 823 K for 8 h in air the mesoporous SBA-3 was finally obtained. In case of niobium-containing samples heteroatom source (niobium(V) chloride (Aldrich) or ammonium trisoxalate complex of niobium (CBMM Brazil)) was dissolved in acidic medium before adding CTAB.

The symbols of the catalysts are as follows: NbSBA-3-$x(y)$ where: $x$ stands for Si/Nb ratio, $y$ defines Nb source: (ox), Nb(V) oxalate; (Cl), Nb(V) chloride; (Co), Nb(V) ammonium trisoxalate complex.

### 2.2. Characterization techniques

#### 2.2.1. Chemical analysis

The niobium content in the calcined NbSBA-3 samples were determined by inductively coupled plasma emission spectroscopy (ICP) (AES-Flammes Perkin-Elmer M 1100) after solubilization of the samples in $H_2SO_4$:$HNO_3$:HCl solutions.

#### 2.2.2. $N_2$ adsorption/desorption

The surface areas and pore volumes of the NbSBA-3 materials were measured by nitrogen adsorption at 77 K using the conventional technique on a Micromeritics ASAP 2010 apparatus. Prior to the adsorption measurements, the samples were degassed in vacuum at 573 K for 2 h. The specific surface area was evaluated with the BET method, and the pore diameter from the adsorption branch of isotherms using a corrected algorithm (KJS-BJH) [11]. External and total surface area, mesopores and total pore volume were calculated using $\alpha_S$ plot method.

#### 2.2.3. X-ray diffraction study

Powder X-ray diffraction (XRD) patterns were recorded between 1° and 40° ($2\theta$) on a Bruker (Siemens) D5005 diffractometer (Cu Kα radiation; λ = 0.15418 nm) with a 0.02° step size.

#### 2.2.4. UV–vis spectroscopy

UV–vis spectra were obtained in a Perkin-Elmer Lambda 9 spectrometer equipped with a reflectance accessory and a homemade sample holder containing 0.2 g solid powder. $BaSO_4$ was used as a reference in the measurements.

#### 2.2.5. FTIR acidity measurements

Infrared spectra were recorded with a Brucker Vector 22 FTIR spectrometer (DTGS detector). Pyridine was used as basic probe. The samples were pressed under low pressure, into a thin wafer ~10–15 mg $cm^{-2}$ and placed in the vacuum cell. The activation was performed first in a flow of $O_2$ at 723 K for 1 h. Next, $O_2$ was evacuated at room temperature (RT). After that, the sample was outgased at 673 K for 12 h. Pyridine was adsorbed at 373 K. The desorption was carried out for 30 min at each of the following temperatures: 373, 423, 473, 523, and 573 K. All spectra were recorded at room temperature. The spectra shown in this paper are recalculated for the same weight of the samples, 1 mg.

### 2.3. Catalytic tests

#### 2.3.1. Gas phase oxidative dehydrogenation (ODH) of propane

The reactions were carried out using a conventional fixed-bed flow reactor (diameter 16 mm) working at atmospheric pressure. One cubic centimetre of the catalyst was loaded into a U-type reactor made of quartz tube and treated in flow of $N_2$ (40 $cm^3$ $min^{-1}$) at 823 K for 4 h before the reaction. The reactor was equipped with a coaxial thermocouple for catalytic bed temperature profiling. The feed consisted of a mixture of propane/oxygen/nitrogen with a molar ratio 7/13/80 and a total gas flow of 17.5 $cm^3$ $min^{-1}$. Catalytic experiments were carried out in the 753–823 K temperature range. In these conditions, both external and internal diffusion limitations were absent. The substrate and products were analyzed by Shimadzu GC-14B gas chromatograph with FID detector equipped with three columns: Durapak (for hydrocarbons separation), Carbowax 20 M and AT1200 (for oxygenates separation) and Delsi GC 121MB chromatograph with TCD detector using Tamis 5A (for $O_2$, $N_2$, CO) and Porapak Q (for $CO_2$, $H_2O$). Carbon balance was kept within 5% or below.

#### 2.3.2. Liquid phase oxidation of cyclohexene with $H_2O_2$

All prepared materials were tested in the oxidation of cyclohexene with hydrogen peroxide. The reaction was performed at 318 K in the liquid phase using acetonitrile as a solvent. The catalytic reaction between cyclohexene and hydrogen peroxide was carried out in a glass flask equipped with a magnetic stirrer, a thermocouple, a reflux condenser, and a membrane for sampling. 0.04 g of a calcined catalyst was placed into the flask where the solvent was added. The oxidation was conducted simply by efficient stirring of a mixture of a solvent and a catalyst at 318 K. After stirring for 15 min, cyclohexene (2 mmol) was added, followed by the dropwise addition of ~34% hydrogen peroxide (2 mmol). The first analysis was done after 30 min from the beginning of the reaction. Samples were taken at regular time intervals and analyzed by a gas chromatograph GC 8000 Top equipped with a capillary column of DB-1, operated with a heating program: 333 K for 15 min, ramp 10 K $min^{-1}$ to 353 K (kept for 13 min), attached to a FID.

## 3. Results

### 3.1. Characterization of the catalysts

The composition of the materials indicated as assumed and real atomic Si/Nb ratios is shown in Table 1. This table contains also the data from our previous papers [3,5] concerning NbSBA-15 and NbMCM-41 samples. The isomorphous substitution of silicon in SBA-3 with niobium strongly depends

Table 1
Catalysts, their compositions and number of LAS

| Catalysts[a] | Assumed atomic ratio Si/Nb | Real atomic ratio Si/Nb | Number of LAS ($\times 10^{17}$)[b] | References |
|---|---|---|---|---|
| NbSBA-3-32(Co)[c] | 32 | 113 | – | This work |
| NbSBA-3-32(Cl)[d] | 32 | 24 | 222 | This work |
| NbSBA-3-64(Cl)[d] | 64 | 52 | 181 | This work |
| NbSBA-3-128(Cl)[d] | 128 | 107 | 93 | This work |
| NbSBA-15-32(ox)[e] | 32 | 73 | 41 | [5] |
| NbSBA-15-128(ox)[e] | 128 | 207 | 170 | [5] |
| NbMCM-41-32(ox)[e] | 32 | 26 | 158 | [3] |

[a] The last number in catalyst symbols denotes Si/Nb assumed ratio.
[b] Number of LAS calculated per 1 g of the catalyst from IR bands obtained after pyridine adsorption and desorption at 373 K ($\varepsilon_{1450} \approx 1.5$ μmol$^{-1}$ [12]).
[c] Nb(V) ammonium trisoxalate complex.
[d] Nb(V) chloride.
[e] Nb(V) oxalate.

on the metal source, as evidenced from the data in Table 1 (see the difference in Si/Nb assumed and real ratios). The use of Nb(V) chloride allows the introduction of a little higher amount of niobium in relation to silicon than assumed one. A similar phenomenon has been also found in the preparation of other metal containing mesostructured solids, e.g. NbMCM-41 with rather high content of metal [3] or CoMCM-41 [13]. Much lower Si/Nb ratios in NbSBA-3(Cl) and NbMCM-41-32(ox) than in the gels indicates that not all of siliceous atoms used in the synthesis are located in the final samples. However, contrary to NbMCM-41 materials (Si/Nb = 32 or 64), all NbSBA-3 samples prepared within this work are free from the extra framework niobium-oxide phases. XRD patterns in a high-angle range do not show any crystalline phase in case of all NbSBA-3 samples suggesting the location of niobium only in the walls of mesoporous materials.

The other characteristic is noted in the case of NbSBA-3-32(Co) prepared from ammonium trisoxalate complex used as Nb source. The real Si/Nb ratio is much higher than that in the gel, indicating that only a part of niobium atoms are included into the walls (no extra framework Nb species was detected by XRD). Interestingly, a similar feature was found earlier in NbSBA-15-32(ox) and NbSBA-15-128(ox) synthesized in the presence of niobium oxalate as Nb source [5]. However, in this case extra framework $Nb_2O_5$ phase was estimated from the XRD patterns. These results suggest that bulky molecules of niobium oxalate or ammonium trisoxalate complex do not easy substitute silicon when the synthesis is performed in acidic medium. Under an alkaline conditions used in the preparation of NbMCM-41-32(ox) much higher isomorphous substitution of silicon by niobium occurs.

### 3.2. X-ray diffraction and low-temperature nitrogen adsorption

The textural properties of NbSBA-3 materials were estimated on the basis of low-angle XRD patterns (Fig. 1A) and $N_2$ adsorption/desorption isotherms (Fig. 1B). The data are summarized in Table 2. All the NbSBA-3 solids exhibit a well ordered 2d hexagonal mesoporous structure typical of SBA-3 materials deduced from XRD peaks. $N_2$ adsorption/desorption isotherms are shown in Fig. 1B for the samples prepared from Nb ammonium trisoxalate complex (isotherm a) and Nb chloride (isotherm b) exhibiting Si/Nb = 32 assumed ratio. They are of type IV according to the IUPAC classification. Only the first material shows a small hysteresis loop, whereas the second one, as well as all other samples (not shown in the figure) prepared from Nb chloride, do not show any hysteresis loop. As the relative pressure increases to c.a. $p/p_0 \approx 0.15$ all isotherms show a sharp step characteristic of capillary condensation of nitrogen within uniform mesopores. Uniformity of mesopores is well visible in pore size distribution (PSD) curves (Fig. 1C) which are almost the same for all NbSBA-3 samples. The other textural parameters differ more or less depending on the Nb content and Nb source used in the synthesis. In case of NbSBA-3 samples prepared from niobium(V) chloride BET surface area as well as external and total surface area calculated from $\alpha_S$ plots, mesopores and total pore volume, and $d_{1\,0\,0}$ values increase with the decrease of Nb content in the material (from Si/Nb = 32–128 as assumed). All these parameters are slightly higher when the material is synthesized in the presence of Nb ammonium trisoxalate complex.

### 3.3. Metal location

UV–vis spectra (Fig. 2) allow the estimation of niobium tetrahedrally coordinated and linked to a silica surface (a band at c.a. 220 nm) and octahedral $Nb_2O_5$ giving rise to a band at c.a. 330 nm (Fig. 2 a) [5,14]. The UV band at c.a. 220 nm is well distinguished in case of both samples exhibiting assumed Si/Nb = 32 (Fig. 2b and c). It is shifted to the lower wavelength when the Si/Nb is much higher (less niobium species). Only NbSBA-3-32(Cl) shows the tail at a higher wavelength (Fig. 2 b) which could cover the small band due to $Nb_2O_5$ species (if any). However, the presented UV–vis spectra do not show clearly the presence of extra framework $Nb_2O_5$ phase. For comparison UV–vis spectrum of $Nb_2O_5$ is included. Moreover, NbSBA-3-32(Co) shows the lack of the mentioned earlier tail indicating that the only position for Nb is its location linked to a silica surface and tetrahedrally coordinated.

### 3.4. Acidity measurements

Pyridine adsorption on the catalyst surfaces followed by FTIR measurements give an informative data concerning

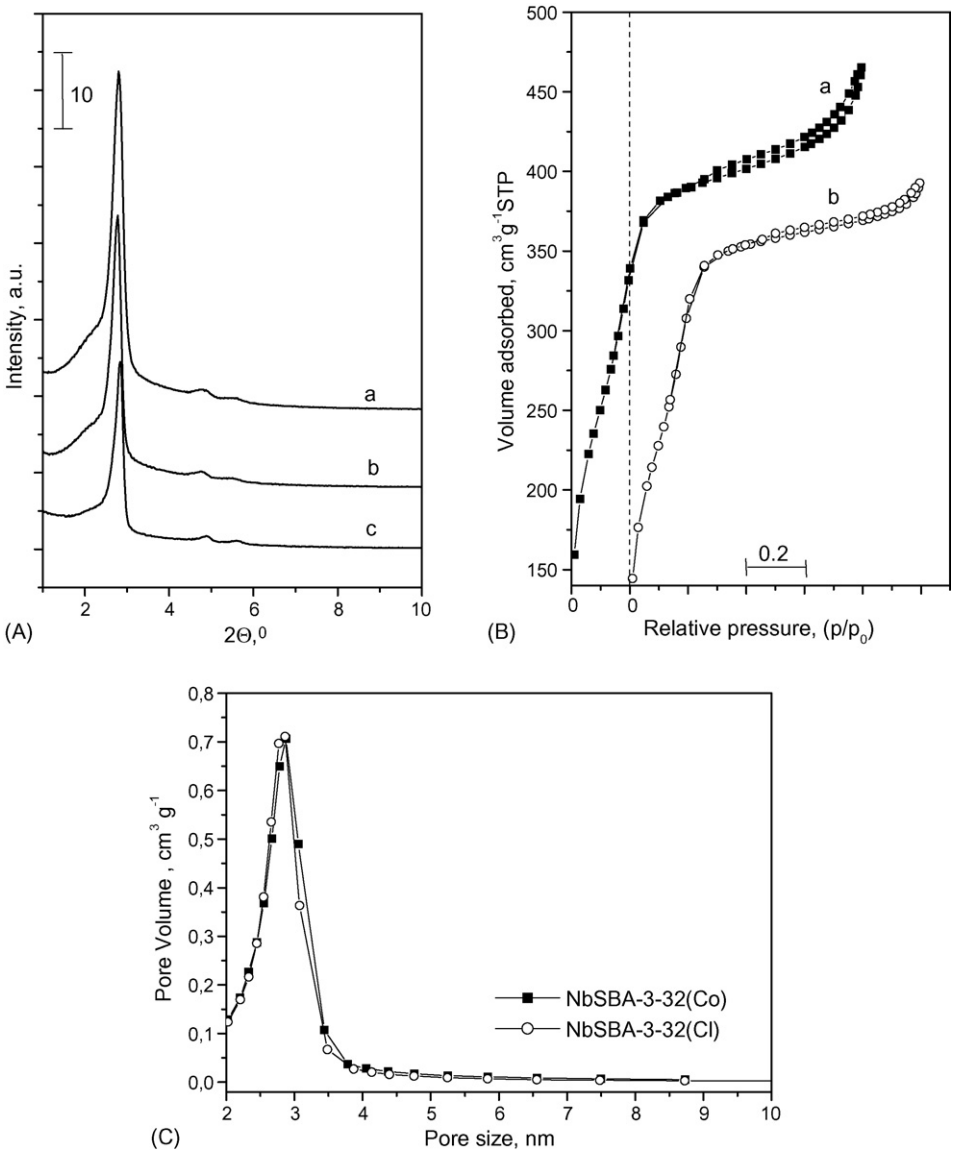


Fig. 1. (A) XRD patterns of calcined SBA-3 materials: (a) SiSBA-3, (b) NbSBA-3-32(Co), (c) NbSBA-3-32(Cl); (B) low temperature nitrogen adsorption/desorption isotherms: (a) NbSBA-3-32(Co), (b) NbSBA-3-32(Cl); (C) pore size distribution.

acidity of the solids. Using this method one can estimate the nature of acidic centres (Brønsted or Lewis) and their concentration. Pyridine (p$K_b$ 8.8) interacts with Lewis acid sites (LAS) giving rise to characteristic IR bands at ~1610 ($\upsilon_{8a}$ mode) and ~1445 $cm^{-1}$ ($\upsilon_{19b}$ mode). The intensity of the $\upsilon_{19b}$ band is related to the number of LAS taking into account that $\varepsilon_{1450} \approx 1.5\ \mu mol^{-1}$ [12]. The FTIR studies of pyridine adsorbed at 373 K followed by 30 min desorption at the same temperature allow us to estimate Lewis acidity of the catalysts. Fig. 3 compares chemisorption of pyridine on NbSBA-3

Table 2
The textural properties of NbSBA-3 materials

| Catalysts | Surface area ($m^2\ g^{-1}$) | | | $V_{meso}$ ($cm^3\ g^{-1}$)[b] | $V_{tot}$ ($cm^3\ g^{-1}$)[b] | PD (nm) | $d_{1\,0\,0}$ (nm) |
|---|---|---|---|---|---|---|---|
| | BET[a] | $S_{ext}$[b] | $S_{tot}$[b] | | | | |
| NbSBA-3-32(Co) | 1139 | 107 | 1097 | 0.552 | 0.708 | 2.88 | 3.19 |
| NbSBA-3-32(Cl) | 1050 | 55 | 992 | 0.524 | 0.602 | 2.87 | 3.11 |
| NbSBA-3-64(Cl) | 1087 | 66 | 1093 | 0.541 | 0.648 | 2.86 | 3.12 |
| NbSBA-3-128(Cl) | 1137 | 75 | 1094 | 0.558 | 0.673 | 2.86 | 3.13 |

[a] Calculated in the range $p/p_0 = 0.05$–$0.15$.
[b] Calculated using $\alpha_S$ plot method.

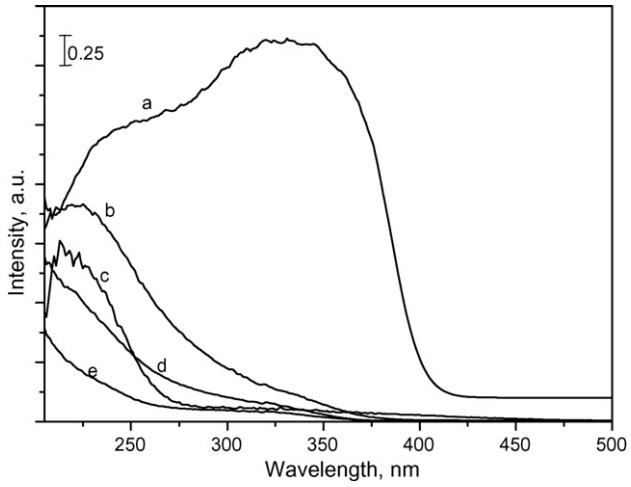


Fig. 2. UV–vis spectra of: (a) $Nb_2O_5$, (b) NbSBA-3-32(Cl), (c) NbSBA-3-32(Co), (d) NbSBA-3-64(Cl), and (e) NbSBA-3-128(Cl).

samples with various niobium contents. The stability of chemisorbed pyridine can be referred to the strength of Lewis acid sites and can be estimated on the basis of FTIR spectra after evacuation at various temperatures. It is clearly evidenced that the higher niobium contents, the higher strength of Lewis acid sites. The infrared band due to pyridine coordinative bonded to Lewis acid sites diminishes at a lower evacuation temperature when the concentration of niobium is low (Si/Nb = 128), Fig. 3C. The growth of Nb content causes the stronger interaction with pyridine resulting in the higher temperature necessary for its desorption.

It is worthy of notice that no bands from pyridine adsorbed on Brønsted acid sites (lack of the bands at 1640 and 1546 $cm^{-1}$) are detected indicating the presence of only one type of acidity Lewis one. The bands at ~1575 $cm^{-1}$ origin from weak Lewis-bounded pyridine whereas those at 1445 and 1596 $cm^{-1}$ characterize hydrogen-bounded pyridine. Taking into account an extinction coefficient ($\varepsilon_{1450} \approx 1.5$ $\mu mol^{-1}$ [12]) for an IR band at ~1450 $cm^{-1}$ one can calculate the number of Lewis acid sites (LAS) (Table 1). The decrease of Nb species results in the decrease of LAS. There is linear relationship between the real Si/Nb atomic ratio and the number of LAS in NbSBA-3 (Fig. 4). This phenomenon is not true in the case of NbSBA-15 [5] in which a part of Nb species occupies extra framework positions and this material contains also micropores, which can limit the interaction of pyridine with active species. Moreover, the presence of Nb extra framework species in NbSBA-15 disturbs pyridine adsorption on the active centres and therefore interferences the final value of pyridine adsorption. One cannot distinguish pyridine adsorbed on Nb framework species and that on extra framework one.

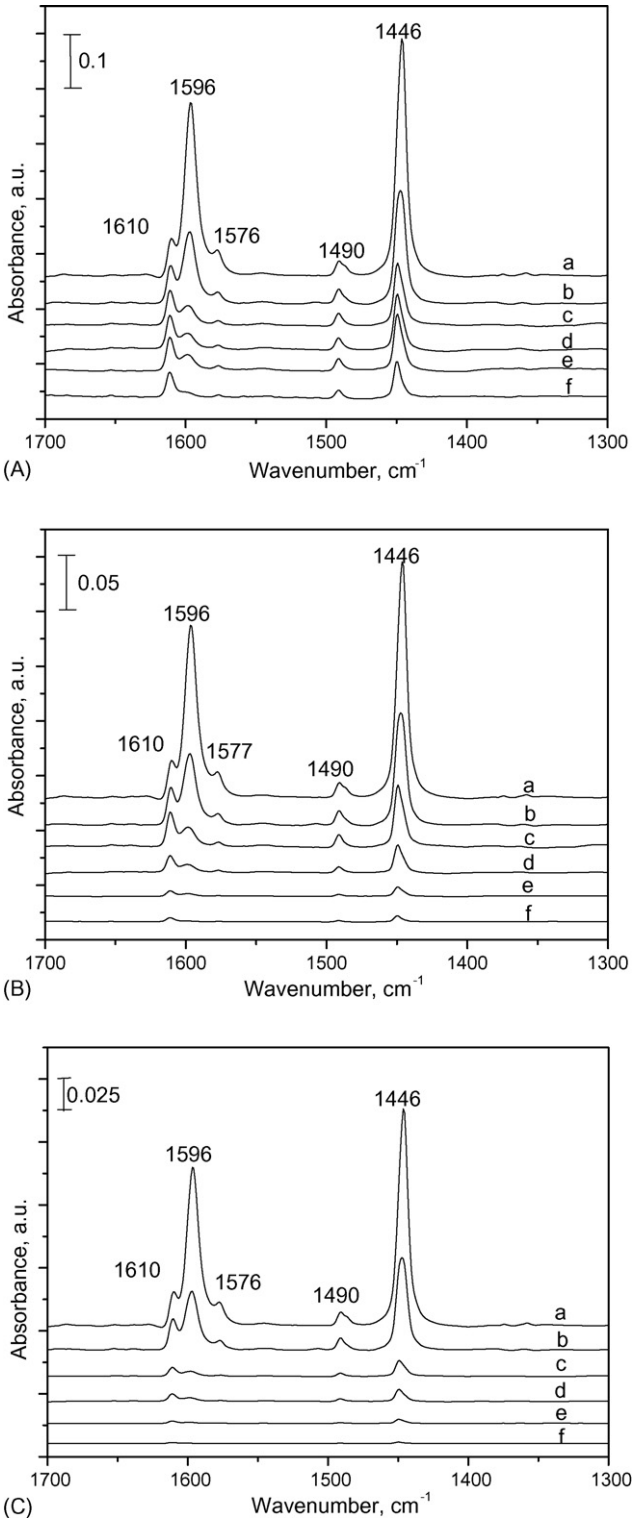


Fig. 3. FTIR spectra recalculated to 1 mg of the materials: (A) NbSBA-3-32(Cl); (B) NbSBA-3-64(Cl); (C) NbSBA-3-128(Cl) after adsorption of pyridine at 373 K (a) and desorption at 373 K (b); 423 K (c); 473 K (d); 523 K (e); 573 K (f).

### 3.5. Catalytic tests

#### 3.5.1. Catalytic activity in oxidative dehydrogenation of propane

Catalytic data for propane ODH on NbSBA-3 samples and the results from our earlier studies on NbMCM-41 and NbSBA-15 are shown in Table 3. The results are compared for approximately 6% propane conversion reached at various temperatures (753–848 K) depending on the catalysts. The stability of the reaction is obtained after c.a. 1 h time on stream.

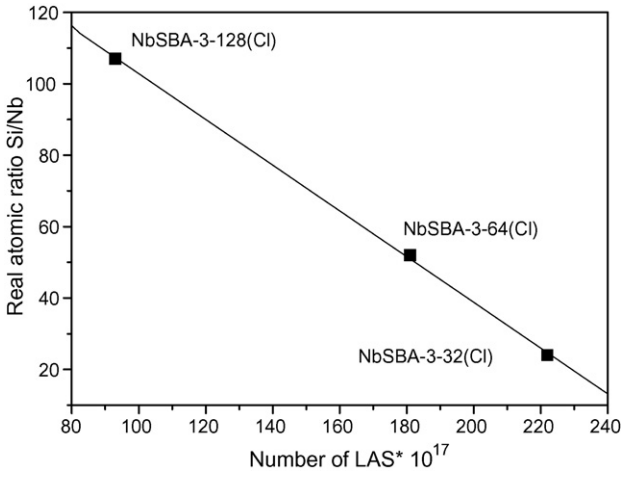


Fig. 4. Relationship between Lewis acidity and real atomic ratio Si/Nb ($\varepsilon_{1450} \approx 1.5\ \mu mol^{-1}$ [12]).

Propene, CO, $CO_2$, and slightly amounts of other hydrocarbons denoted $C_xH_y$ were registered in the reaction products. The main product for all Nb-containing materials is propene (resulted from oxidative dehydrogenation process). However, SiSBA-3 material exhibiting high activity converts propane with a high selectivity to $CO_2$ indicating that the totally combustion of hydrocarbons mainly occurs. Therefore, there is no doubt that niobium species is responsible for the selectivity in the ODH reaction.

The highest selectivity to propene (>80%) was reached on the following samples NbSBA-3-64(Cl), NbSBA-3-128(Cl), NbSBA-15-128(ox). However, in the latter case the activity is lower because for obtaining ~6% conversion of propane the reaction temperature had to be much higher (803 K instead of 773 K for NbSBA-3 samples). Thus, it is clear that NbSBA-3 materials prepared with using niobium(V) chloride as Nb precursor appears as the most attractive catalysts for the propane ODH process among all other Nb-containing mesostructured solids which have been applied for this reaction up to now. Considering selectivity to propene obtained on NbSBA-3(Cl) materials one can conclude that the decrease of Nb species enhances the production of $C_3H_6$. The same phenomenon was found in case of NbMCM-41 samples [3].

It is interesting to notice that two NbSBA-3 materials prepared with using various Nb sources (NbSBA-3-32(Co) and NbSBA-3-128(Cl)) and exhibiting similar Si/Nb real ratios (113 and 107, respectively) show various activity and propene selectivity. The most active and selective catalyst is that prepared from Nb(V) chloride and containing the lowest number of Nb species (i.e. NbSBA-3-128(Cl)). This observation clearly indicates the role of niobium source in the formation of active mesostructured catalysts.

Taking into account the propane conversion at the same reaction temperature on mesoporous molecular sieves prepared in this work and those published elsewhere [3,5] and containing assumed Si/Nb = 32 and 128 ratios one can consider the role of the synthesis conditions on the activity of final materials (Table 4). There is no doubt that NbSBA-3 type solids prepared in acidic medium from niobium(V) chloride present the highest activity. The other material synthesised at the same conditions but with the use of Nb(V) ammonium trisoxalate complex instead of chloride (hexagonal *p6m* NbSBA-3-32(Co)) is also active, even more than micro-mesoporous structured NbSBA-15 prepared also in acidic medium or 2d hexagonal *p6m* NbMCM-41 sample synthesized in basic medium. One should remember, that both NbSBA-15 and NbMCM-41 contained niobium extra framework species contrary to NbSBA-3 solids. Thus, not only reaction media and a type of template used determine the activity of final materials but also the nature (type of anion) of metal salt used as a precursor. A comparison of propane conversion between the samples possessing similar Si/Nb real ratios gives rise to the following relations: NbSBA-3-128(Cl) > NbSBA-3-32(Co); NbSBA-3-32(Cl) > NbMCM-41-32(ox); NbSBA-3-64(Cl) > NbSBA-15-32(ox).

### 3.5.2. Oxidation of cyclohexene

The reaction was performed in the liquid phase and acetonitrile as the reaction medium. Approximately thiry-four percent of hydrogen peroxide was an oxidising agent. Usually, when the reaction is carried out in the liquid phase, the question arises whether it is a homogenous or heterogeneous process. This question was answered previously by performing special experiments [3,15]. The reaction carried out under homogenous conditions (by dissolving of the same amount of niobium salt in acetonitrile, than that used for the catalyst preparation) proceeds with very low activity and high selectivity to cyclohexanediol.

The results of cyclohexene oxidation with hydrogen peroxide on the catalysts prepared within this work and those

Table 3
Propane conversion and selectivity to propene for propane ODH (after 1 h time on stream)

| Catalysts | Reaction temperature (K) | $C_3H_8$ conversion (%) | Selectivity (%) | | | | $C_3H_6$ yield (%) | References |
|---|---|---|---|---|---|---|---|---|
| | | | $C_3H_6$ | CO | $CO_2$ | $C_xH_y$ | | |
| SiSBA-3 | 753 | 6.1 | 26.9 | 0 | 71.1 | 2.0 | 1.6 | This work |
| NbSBA-3-32(Co) | 803 | 6.7 | 79.6 | 3.2 | 14.2 | 3.0 | 5.3 | This work |
| NbSBA-3-32(Cl) | 773 | 6.6 | 77.4 | 2.9 | 17.8 | 1.9 | 5.1 | This work |
| NbSBA-3-64(Cl) | 773 | 6.4 | 82.3 | 2.5 | 13.2 | 2.0 | 5.3 | This work |
| NbSBA-3-128(Cl) | 763 | 6.5 | 86.2 | 1.8 | 10.2 | 1.8 | 5.6 | This work |
| NbSBA-15-32(ox) | 848 | 6.0 | 56.4 | 21.3 | 18.2 | 4.1 | 3.4 | [5] |
| NbSBA-15-128(ox) | 803 | 6.0 | 87.4 | 0 | 8.9 | 3.7 | 5.2 | [5] |
| NbMCM-41-32(ox) | 813 | 6.6 | 55.1 | 13.2 | 31.7 | 0 | 3.6 | [3] |

Table 4
Activity for ODH of propane at 813 K (after 1 h time on steam)

| Catalyst | Real atomic ratio Si/Nb | Propane conversion (%) | References |
|---|---|---|---|
| NbSBA-3-32(Co) | 113 | 9.8 | This work |
| NbSBA-3-32(Cl) | 24 | 15.3 | This work |
| NbSBA-3-64(Cl) | 52 | 9.8 | This work |
| NbSBA-3-128(Cl) | 107 | 13.8 | This work |
| NbSBA-15-32(ox) | 73 | 2.8 | [5] |
| NbSBA-15-128(ox) | 207 | 7.4 | [5] |
| NbMCM-41-32(ox) | 26 | 6.6 | [3] |

published earlier [3,5] are summarized in Table 5. Only in the case of NbSBA-3 materials, in which Nb is located in the skeleton of the samples with tetrahedral coordination, TOF calculations made sense because in the case of other samples various location and various Nb species were concluded.

Taking into consideration maximum conversion and epoxide selectivity it is clearly seen the best performance of NbSBA-3-32(Cl) sample. Although the number of Lewis acid sites, which could recombine with water toward Brønsted acid centres (BAS), is the highest in this material, the selectivity to epoxide is very high. It is known [15] that the presence of BAS causes the ring opening in epoxide and transforms this product into diols. However, the reaction curves plotted in Fig. 5 indicates that the decrease of epoxide selectivity with the reaction time is much slower than that for the other catalysts [3]. Thus, considering the efficiency of the epoxidation process one should propose NbSBA-3-32(Cl) catalyst as the most attractive one. Another point is the activity of the catalysts calculated per number of active centres (TOF, turnover frequency). In other words, the consideration of activity of single niobium species is also important in the discussion of the reaction pathways, optimisation of the catalysts, etc. Taking into account the samples prepared from $NbCl_5$ the TOF number increases with the decrease of Nb atoms in the solid. It means that the higher isolation of Nb species improve the efficiency of cyclohexene oxidation. One should remember that the high concentration of metal species could lead to the fast decomposition of $H_2O_2$ [16] not desired for the effective reaction between hydrogen peroxide and cyclohexene.

Interestingly, NbSBA-3-32(Co) exhibits almost twice higher TOF than that for NbSBA-3-128(Cl) in spite of the comparable number of Nb species. This phenomenon stresses the role of oxalate ions in the formation of oxidative active niobium species. Previously, in case of MCM-41 materials, it was indicated that niobium oxalate used in the synthesis is responsible for the formation of defect holes, which play a crucial role in the oxidative activity of the catalyst [3]. These defects were registered by TEM, but only in case of high concentration of Nb (NbMCM-41-32). In the case of this work, a low concentration of Nb species in the final material does not allow the detection of holes in TEM images. However, a small hysteresis loop observed in the $N_2$ adsorption/desorption isotherm of NbSBA-3-32(Co) (Fig. 1B) could suggest the presence of a small amount of defect holes.

## 4. Discussion

Basing on our earlier experiences [3–5] in the preparation of niobium-containing mesostructured catalysts addressed to the gas and liquid phase oxidation processes we have looked for the materials possessing the uniform type of niobium species, which could allow us to correlate the activity and selectivity with well defined location of metal and number of active centres. For that purpose we have followed Stucky et al. [2] procedure in the preparation of 2d hexagonal *p6m* mesoporous structure denoted SBA-3, which is an analogue to MCM-41 materials. The difference in the preparation of both materials consists in the use of various media. Acidic one replaces basic media used in MCM-41 preparation. The results shown in this paper indicate that the use of acidic medium in the synthesis of NbSBA-3 materials increases the efficiency of niobium introduction into the final material, and moreover, what is even more important, the location of Nb species in the walls of the solid. XRD as well as UV–vis spectra did not indicate the presence of niobium species in the extra framework positions. It is true for all NbSBA-3 samples independent of the Nb source used in the synthesis. This feature has an important impact on the catalytic activity. Contrary to the other niobosilicate mesoporous solids, in case of NbSBA-3 materials the diffusion in pores does not limit the liquid phase reaction rate because the channels are free from extra framework phases. Thus, the activity and selectivity can be easier related to the number of Nb species in the walls, Lewis acidity and texture/structure parameters. Because of the homogeneity of Nb species in

Table 5
Results of cyclohexene oxidation at 318 K after 40 h

| Catalysts | Maximum conversion (%) | Selectivity (%) | | | TOF (mol $atm^{-1}$ $s^{-1}$) | References |
|---|---|---|---|---|---|---|
| | | Epoxide | Diol | Others | | |
| SiSBA-3 | 10.3 | 7.8 | 70.7 | 21.5 | – | This work |
| NbSBA-3-32(Co) | 72.5 | 55.8 | 44.2 | 0 | $20.98 \times 10^{-4}$ | This work |
| NbSBA-3-32(Cl) | 81.6 | 70.2 | 29.8 | 0 | $4.68 \times 10^{-4}$ | This work |
| NbSBA-3-64(Cl) | 53.3 | 50.4 | 49.6 | 0 | $7.41 \times 10^{-4}$ | This work |
| NbSBA-3-128(Cl) | 45.4 | 45.0 | 55.0 | 0 | $11.53 \times 10^{-4}$ | This work |
| NbSBA-15-32(ox) | 33.5 | 35.5 | 64.5 | 0 | – | [5] |
| NbSBA-15-128(ox) | 16.3 | 31.8 | 68.2 | 0 | – | [5] |
| NbMCM-41-32(ox) | 75.5 | 57.6 | 24.1 | 18.4 | – | [3] |

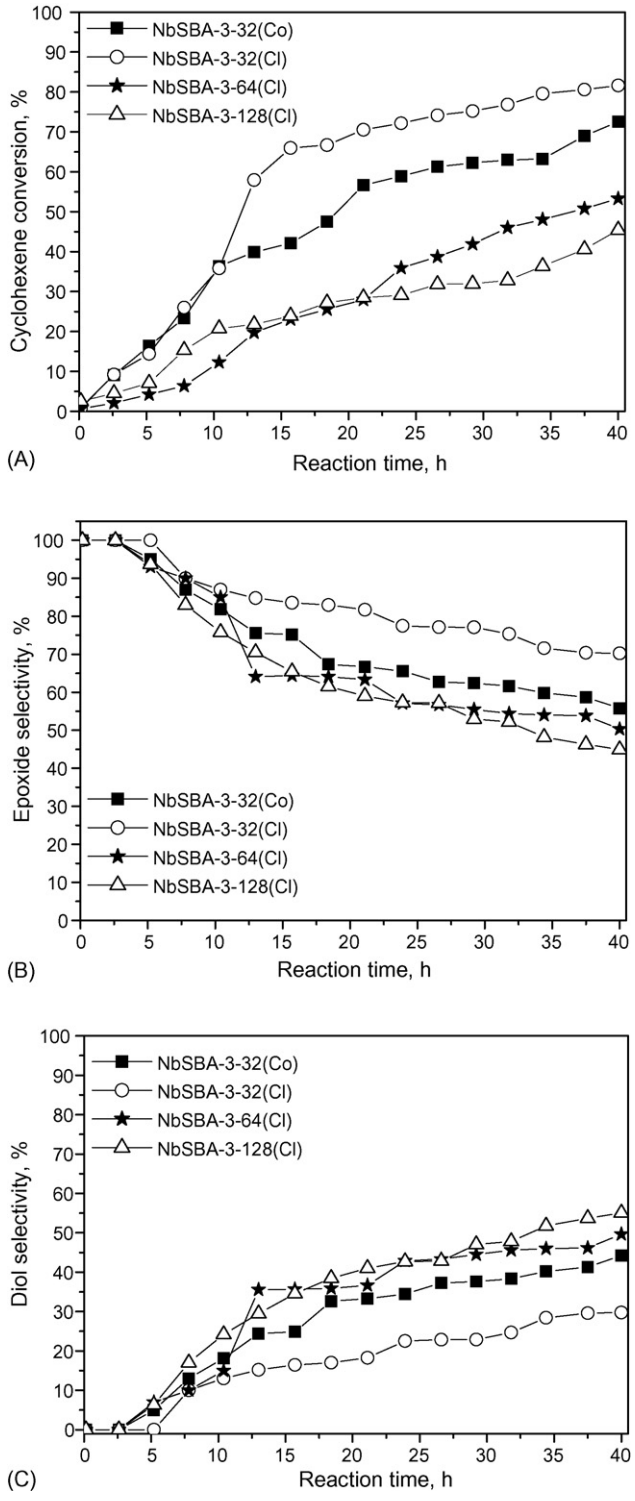


Fig. 5. Activity of the catalysts in the oxidation of cyclohexene with hydrogen peroxide (A) and selectivity to epoxide (B), and diol (C).

these materials, one can correlate the activity and selectivity with the number, strength of active sites, as well as the isolation of Nb species.

The highest strength of niobium species which play a role of Lewis acid sites, determined from pyridine adsorption followed by FTIR spectroscopy measurements (Fig. 3), was observed for NbSBA-3-32(Cl) containing the highest number of niobium species. The propene selectivity in propane ODH process changes in a way different than the estimated acidity showing that for this reaction much important feature is isolation of metal active species. Therefore, due to the location of Nb only inside the walls and the lack of Nb-oxide extra framework species, NbSBA-3 materials are much more attractive for oxidative dehydrogenation of propane than the other NbMCM-41 and NbSBA-15 solids applied up to now in this reaction [3,5]. The presence of extra framework niobium species in the latter materials causes the increase of propane transformation to CO and $CO_2$. The comparison of the ODH results for all three types of mesostructured materials (NbSBA-3, NbMCM-41 and NbSBA-15) (Table 3) and taking into account the defined textural/structural parameters, one can evidence that niobium tetrahedrally coordinated and connected with siliceous-oxygen species in the walls is responsible for the oxidative dehydrogenation of propane towards propene, whereas niobio-oxide species located in the extra framework sites are responsible for the oxidation of hydrocarbons towards CO and $CO_2$.

The other interesting founding from this work is the estimation of a role of niobium precursor in the generation of active species. It is very probable that bulky Nb-precursor molecules (like ammonium trisoxalate complex used for NbSBA-3 or oxalate salt applied in the synthesis of NbMCM-41 materials) cause the formation of defect holes in the final materials. This action seems to be more evidence when the synthesis occurs in the basic media. The role of defect holes in the oxidative activity of NbMCM-41 was discussed elsewhere [3].

The preparation of NbSBA-3 free from extra framework niobium species allows the consideration of TOF number for the activity in cyclohexene epoxidation. The obtained results (Table 5) allow us to correlate the activity in this reaction not only with the diffusion efficiency as it was shown in [3] but also with the isolation of active metal species. This isolation avoids too fast decomposition of oxidative agent ($H_2O_2$) and due to that makes the epoxidation reaction more effective in relation to the single active centre.

The results presented in this paper show the significant activity of SiSBA-3 material (without niobium) in both oxidation processes. This feature is on line with the literature data [17–19] indicating oxidizing properties of dehydroxylated silica. Silica activity is related to the surface defects (reduced sites) important for the generation of active oxygen species, which initiates the radical reactions [17] or to the formation of $SiOO^{-}Si$ species involved in the radical type catalytic oxidation [18,19]. Thus, the activity of SiSBA-3 in the cyclohexene oxidation with $H_2O_2$ confirms our earlier suggestion [15] that the radical reaction pathway takes place in case of the use of mesostructured solid catalysts for this process. Very high activity of SiSBA-3 in the propane oxidation (Table 3, reaction temperature 753 K for 6.1% conversion) is accompanied by high selectivity to $CO_2$ (the total combustion product). The presence of niobium in SBA-3 material is necessary for steering the reaction toward propene.

## 5. Conclusions

To the best of our knowledge, this is the first report on the preparation of Nb-Si-mesostructured solids (NbSBA-3) without extra framework Nb-oxide phases located in the mesoporous tubes or outside the walls and their successful application in the gas and liquid phase oxidation. XRD, UV–vis and IR studies allow us to conclude the isomorphous substitution of Si with Nb and the presence of homogeneous Nb species inside the walls. Nb(V) chloride used in the synthesis of NbSBA-3 gave rise to a higher Nb content in the final material than the use of Nb ammonium trisoxalate complex. All NbSBA-3 materials prepared in this work are very attractive catalysts in both oxidative dehydrogenation of propane and epoxidation of cyclohexene. Some of them are more effective in both processes than the corresponding NbMCM-41 and NbSBA-15 catalysts.

## Acknowledgements

Polish State Committee for Scientific Research (KBN, grants 3 T09A 094 27; 2004–2005 and 3 T09A 100 26; 2004–2007) is acknowledged for the financial support. The CBMM Brazil is acknowledged for providing ammonium trisoxalate complex of niobium and niobium oxalate. The authors appreciate Dr. Izabela Nowak for calculations of texture parameters from nitrogen sorption isotherms.

## References

[1] J.S. Beck, J.C. Vartuli, W.J. Roth, M.E. Leonowicz, C.T. Kresge, K.D. Schmitt, C.T.-W. Chu, D.H. Olson, E.W. Sheppard, S.B. McCullen, J.B. Higgins, J.L. Schlenker, J. Am. Chem. Soc. 114 (1992) 10834.
[2] Q. Huo, D.I. Margolese, U. Ciesla, D.G. Demuth, P. Feng, T.E. Gier, P. Sieger, A. Firouzi, B.F. Chmelka, F. Schüth, G.D. Stucky, Chem. Mater. 6 (1994) 1176.
[3] B. Kilos, M. Aouine, I. Nowak, M. Ziolek, J.C. Volta, J. Catal. 224 (2004) 314.
[4] B. Kilos, J.C. Volta, I. Nowak, P. Decyk, M. Ziolek, Stud. Surf. Sci. Catal. 154 (2004) 848.
[5] B. Kilos, I. Nowak, M. Ziolek, A. Tuel, J.C. Volta, Stud. Surf. Sci. Catal. 158 (2005) 1461.
[6] M. Ziolek, I. Sobczak, A. Lewandowska, I. Nowak, P. Decyk, M. Renn, B. Jankowska, Catal. Today 70 (2001) 169.
[7] M. Ziolek, I. Nowak, Zeolites 18 (1997) 356.
[8] X. Gao, I.E. Wachs, M.S. Wong, J.Y. Ying, J. Catal. 203 (2001) 18.
[9] I. Nowak, M. Ziolek, M. Jaroniec, J. Phys. Chem. B 108 (2004) 3722.
[10] I. Nowak, Colloid Surf. A: Physicochem. Eng. Aspects 241 (2004) 103.
[11] M. Kruk, M. Jaroniec, A. Sayari, Langmuir 13 (1997) 6267.
[12] S. Khabtou, T. Chevreau, J.C. Lavalley, Micropor. Mater. 3 (1994) 133.
[13] W.A. Carvalho, P.B. Varaldo, M. Wallau, U. Schuchardt, Zeolites 18 (1997) 408.
[14] M. Nashimura, K. Asakura, Y. Iwasawa, J. Chem. Soc., Chem. Commun. 15 (1986) 1660.
[15] I. Nowak, B. Kilos, M. Ziolek, A. Lewandowska, Catal. Today 78 (2003) 487.
[16] M. Ziolek, Catal. Today 90 (2004) 145.
[17] F. Cavani, F. Trifirò, Catal. Today 51 (1999) 561.
[18] A. Satsuma, N. Sugiyama, Y. Kamiya, T. Hattori, Chem. Lett. (1997) 1051.
[19] Y. Matsumura, K. Hashimoto, J.B. Moffat, J. Phys. Chem. 96 (1992) 10448.